

Received October 30, 2020, accepted December 3, 2020, date of publication December 14, 2020, date of current version December 29, 2020.

Digital Object Identifier 10.1109/ACCESS.2020.3044578

# Multi-Link Scheduling Algorithm of LLC Protocol in Heterogeneous Vehicle Networks Based on Environment and Vehicle-Risk-Field Model

NAN DING<sup>1</sup>, (Member, IEEE), SHAOHUA CUI<sup>1</sup>, CHUANGUO ZHAO<sup>2</sup>, YANHONG WANG<sup>2</sup>, AND BINGCAI CHEN<sup>1</sup>, (Member, IEEE)

<sup>1</sup>Key Laboratory of Intelligent Control and Optimization for Industrial Equipment, College of Computer Science and Technology, Dalian University of Technology, Dalian 116024, China

<sup>2</sup>College of Computer Science and Technology, Dalian University of Technology, Dalian 116024, China

Corresponding authors: Bingcai Chen (china@dlut.edu.cn) and Nan Ding (dingnan@dlut.edu.cn)

This work was supported in part by the National Key Research and Development Program of China under Grant 2018YFB1700102, in part by the National Science Foundation of China under Grant 62072071 and Grant 61803070, in part by the Fundamental Research Funds for the Central Universities under Grant DUT20ZD403 and Grant DUT17RC(3)098, and in part by the Ministry of Military Equipment Development of China under Grant 61402090106.

**ABSTRACT** Heterogeneous vehicle network, which integrates cellular network with dedicated short-range communication network, is an effective solution for meeting the communication requirements of the intelligent transportation system. Aiming at the diversity of network applications and harsh environment, and multiple network physical media fusion demand, this paper mainly puts forward a new link scheduling algorithm in LLC layer (LLCA) based on the vehicle risk estimation and event-triggered mechanism to control and schedule the link resources of heterogeneous vehicle networks. Firstly, after establishing the vehicle-risk-field model and estimating the vehicle risk state, the real-time sending frequency of the WSM data is derived. In order to provide the theoretical basis for data packets to select links, the upper bound of the non-WSM data largest distribution frequency of IEEE 802.11p link is given according to the Pareto optimality. Then, based on the upper bound of the maximum non-WSM distribution frequency and IEEE 802.11p link, LLCA algorithm is designed. Meanwhile, the theoretical analysis of time complexity of the algorithm is implemented. Finally, the simulation results show that the proposed LLCA not only reduces the transmission delay of WSM data for secure applications, but also improves the utilization of links on the premise of satisfying most of the QoE network applications.

**INDEX TERMS** Heterogeneous vehicle networks, link scheduling, Pareto optimality, vehicle-risk-field.

## I. INTRODUCTION

The heterogeneous vehicle network, a network for information exchange in the Internet of Vehicles (IoV) among on-board unit (OBU) on vehicles, road side unit (RSU) and the cloud platform, plays an important role in improving the performance of the transportation system of the city [1], [2]. As a major industrial cyber-physical systems (ICPS), wireless communication technologies widely used in IoV including Wi-Fi, WiMAX, IEEE 802.11p, LTE and 5G [3], [4]. WAVE protocol is proposed by the United States, which is used for the standard communication protocol between vehicles and vehicles (V2V), vehicles and road

side infrastructure (V2I) [5]. The standard architecture of WAVE protocol is shown in Figure 1. IEEE 802.11p is used as the bottom transmission protocol in WAVE standard protocol stack. Different from the traditional TCP/IP protocol, WAVE adds IEEE 1609.3 WSMP protocol in the network layer, which is specially used to deal with the wireless short message (WSM) related to the safe driving of vehicles [6]. WSM is related to the safe driving of vehicles, so that higher transmission requirements are needed.

At present, the application demand of IoV is growing, and it is difficult to meet the actual demand only using a single wireless network access technology [7]. In order to improve the reliability and robustness of IoV networks, it is necessary to combine a variety of wireless communication technologies to realize the construction of IoV [8]. By integrating multiple

The associate editor coordinating the review of this manuscript and approving it for publication was Qilian Liang<sup>1</sup>.

|        |               |      |
|--------|---------------|------|
| 1609.3 | UDP/TCP/Other | WSMP |
|        | LLC           |      |
| 802.11 | WAVE MAC      |      |
|        | PHY           |      |

FIGURE 1. WAVE standard protocol stack.

network interfaces on the vehicle terminal, a variety of network resources can be reasonably utilized [9], [10]. However, data transmission is still based on TCP/IP protocol in the current network convergence framework, and there is still a lack of data content-oriented distribution strategy [11], [12].

According to the data content and considering the impact of harsh environmental factors, improving the transmission rate of WSM and the QoE of security services, while ensuring the QoE of non-security services, are the challenges faced by the integration of heterogeneous networks [13].

Aiming at the above problems, this paper introduces the concept of energy field to describe the risk filed intensity of vehicle driving which can be seen as a special triggered rule, and controls the transmission frequency of WSM data according to the risk field intensity, so as to optimize network resource scheduling and improve channel utilization on the premise of ensuring vehicle driving safety.

The innovation of this paper is mainly reflected in the following three aspects.

- 1) Based on the physical phenomenon of field energy, the relationship among the vehicles speed, distance and the frequency of safety information transmission is presented, which provides the basis for adjusting the network resource optimization.
- 2) It is first time that the vehicle risk field model is introduced for vehicle communication. The risk filed intensity of vehicle is described by both of the vehicle speed  $V$  and relative distance  $D$  with a solid theoretical basis.
- 3) In this paper, Pareto optimality theory is used to analyze the upper bound of the non-WSM (NWSM) largest distribution frequency.

## II. RELATED WORKS

Recently, the continuous upgrading of network hardware and the emergence of 5G network present a stringent requirement for the data transmission rate of the underlying hardware [14]. Thus, many researchers begin to use network functions virtualization (NFV) technology to improve network protocol, manage and use network resources, to realize the heterogeneous network integration of IoV [15]. Till now, most of the improvement of network protocol is aimed at one layer of five-layer network protocol stack [16], [17].

In reference [8], a QUVoD architecture is proposed featuring to the integration of 4G, VANET, and a QXIP module in

the IP layer. Due to its intelligent data distribution function, the QXIP can select appropriate links for data transmission according to the quality parameters of different links, such as RTT, packet loss rate and throughput, to integrate and manage the two networks. In reference [13], a concept of Het-VNETs is proposed and a Heterogeneous Link Layer (HLL) is added to Mac layer to realize the network integration of IoV. HLL can shield the details of the lower layer, provide a unified interface for the upper layer, and adapt to different wireless access technologies of the lower layer. It is noticeable that, in reference [8], a network resource scheduling optimization method is designed. Based on the queuing scenario of driverless vehicles, the transmission frequency is automatically adjusted according to the distance between vehicles, and the number of safety information transmission is increased on the premise of ensuring the normal transmission of safety information.

Risk field is an effective evaluation method of vehicle driving safety assistance. Modern driving risk evaluation method combines mathematics, physics, Artificial Intelligence (AI) and other theories to study [18]. In recent years, some scholars have introduced the artificial potential energy field model to describe the vehicle movement risk, established the potential energy function, and compared the driving risk by the potential energy size [19]. A model based on the concept of gravitational field is proposed to describe the behavior relationship between the target vehicle and the surrounding vehicle with the help of gravity and repulsion [20]. A spring model is established, which assumes that a virtual potential energy field is formed by the spring link between vehicles. The risk field intensity of vehicles is determined by analyzing the force model [21]. The electric field model is introduced to simulate the vehicle as a particle with the same charge, the risk field of the vehicle as an electric field generated by particles, and the risk of the vehicle driving in the risk field as an electric field force received by particles in the electric field [22]. On this basis, the risk field model of the influence of the three factors of human vehicle road is proposed, which is applied to the vehicle collision avoidance problem. In 2017, Intel Corporation put forward RSS (responsive sensitive safety) technology, which determines the safety distance based on the factors such as front vehicle speed, rear vehicle speed, driver response time, minimum brake acceleration, maximum brake acceleration, etc., to achieve collision warning [23]. In 2019, NVIDIA company proposed the SFF (the safety force field) model, through the driving data collected by sensors, considering the factors such as vehicle steering, braking, etc., using the mathematical model to establish an equivalent "safety force field" in front of the vehicle, to achieve the purpose of avoiding collision [24].

To summarize, most of the current work is only improved based on the traditional TCP/IP protocol [25], lack of network resource management and optimization for security related data packets, such as WSM packets. To solve the above problems, this paper uses the vehicle risk field to judge the driving state of the vehicle, and designs the link scheduling

algorithm for the LLC layer to realize the mixed transmission of safe and unsafe data messages (WSM and NWSM) in heterogeneous networks. The specific algorithm and protocol architecture are shown in Figure 2.

|                                 |                  |                  |
|---------------------------------|------------------|------------------|
| TCP/UDP                         |                  | IEEE 1609.3 WSMP |
| IPv6                            |                  |                  |
| LLC (Link scheduling algorithm) |                  |                  |
| MAC LTE                         | MAC IEEE 802.11p | ...              |
| PHY                             | PHY              | ...              |

FIGURE 2. LLCA and vehicle protocol structure.

### III. LINK STATE EVALUATION MODEL

#### A. VEHICLE RISK FIELD MODEL

In this paper, the electric field model is chosen to describe the risk of vehicles. As shown in Figure 3, considering the current vehicle 0 to be the reference system, a vehicle risk field model is established. Because there is interaction between vehicle and vehicle, vehicle and object, its function can be regarded as a kind of “physical field”, like charge field. Vehicle and object can be regarded as charged charge, and each charge will be affected by other charges, which is expressed as electric field force. Its formula is as follows:

$$F = \frac{kq_1q_2}{r^2} \quad (1)$$

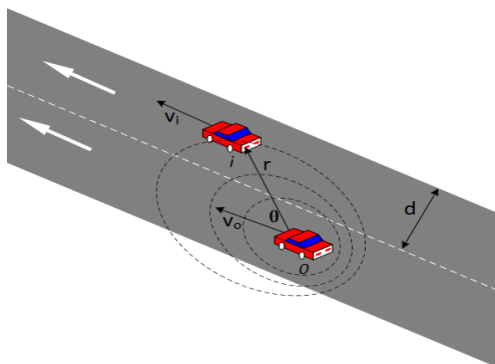


FIGURE 3. Schematic diagram of vehicle risk field.

where  $q_1, q_2$  is the amount of charge of the two charges, and  $r$  is the distance between them.  $k$  is a constant called electrostatic force constant and  $k = 9.0 \times 10^9 \text{ Nm}^2/\text{C}^2$ .  $F$  is the force on the charge in the electric field.

Similarly, the interaction between vehicles can be regarded as the action of force, and the risk field is used to describe the field of vehicle running state. The charge field is used to describe the vehicle risk field of vehicles. The objects on the road generally include vehicles, obstacles, pedestrians, etc.

The vehicle risk field is determined by the object type and speed. When an object is moving, the distribution of vehicle risk field is different from when it is stationary. From practical experience, the risk level in front of the moving object is greater than that is in the rear, as shown in Figure 3, which is similar to the Doppler effect. Doppler effect refers to the change of the wavelength of the object radiation due to the relative motion of the source and the mover. In front of the moving wave source, the wavelength becomes shorter and the frequency becomes higher; behind the moving wave source, the wavelength becomes longer and the frequency becomes lower.

$$\frac{E'}{E} = \frac{(V_{max} + \cos |V_{0i}|)}{V} = \beta \quad (2)$$

$$\theta = \arcsin(\text{sgn}(\frac{r}{V_{0i}})|\frac{d}{r}|) \quad (3)$$

$$V_{0i} = V_0 - V_i \quad (4)$$

where  $E$  is the risk field intensity when the vehicle is stationary and  $E'$  is the risk field intensity when the vehicle is moving.  $V_{max}$  is the maximum speed allowed for the road, generally  $V_{max} = 40\text{m/s}$ ,  $d$  is the road width,  $r$  is the distance from the current vehicle 0 to the surrounding vehicle  $i$ , with the road direction as the positive direction. When the current vehicle is in front of the surrounding vehicle,  $r$  is positive, and when the current vehicle is at the rear of the surrounding vehicle,  $r$  is negative.  $\theta$  is the angle between  $r$  and the relative velocity  $V_{0i}$  between the current vehicle 0 and the surrounding vehicle  $i$ ,  $\theta \in [0, \pi]$ .  $V_0$  is the speed of current vehicle 0,  $V_i$  is the speed of surrounding vehicle  $i$ .

The model of vehicle risk field is related to vehicle type, vehicle speed and vehicle distance. This information can be obtained in real time through vehicle and road test unit or other vehicle communication.

$m_i$  is defined as the type of vehicle. According to the actual situation, the road moving objects are divided into six types: 1: obstacles, 2: pedestrians, 3: non-motor vehicles, 4: small-motor vehicles, 5: medium-motor vehicles, 6: large-motor vehicles. After normalization, formula (5) is obtained.

$$m'_i = \frac{m_i}{m_i + 1} \quad (5)$$

$$M_i = m'_i V_i^2 \quad (6)$$

When vehicle  $i$  enters the risk field of vehicle 0, vehicle 0 receives the force  $F_{0i}$  from vehicle  $i$ , which is expressed as:

$$F_{0i} = \frac{\beta G M_0 M_i}{r_{0i}^2} \quad (7)$$

where  $G$  is a constant and  $G = 1$ .  $M_i$  is the relative mass of vehicle  $i$ , which is related to vehicle type and vehicle speed.  $r_{0i}$  is the distance from vehicle 0 to vehicle  $i$ .

The relationship between risk power and risk intensity is shown in formula (8), where  $E_0$  is the risk intensity of the risk field of vehicle 0.

$$F_{0i} = E_0 M_i \quad (8)$$

Define  $F_{max}$  as the maximum risk force of the current vehicle:

$$F_{max} = \beta \cdot \frac{GM_0M_i}{s^2} \Big|_{\theta=0} \quad (9)$$

where  $s$  is the minimum safe distance between vehicles, which is related to the current speed of the vehicle. The acquisition method is shown in Table 1.

**TABLE 1. The relationship between safe vehicle distance and driving speed.**

| Driving status | Condition                 | Safety distance |
|----------------|---------------------------|-----------------|
| High speed     | $v > 100km/h$             | $S \geq 100m$   |
| Fast speed     | $70km/h < v \leq 100km/h$ | $S \geq \ v\ $  |
| Medium speed   | $40km/h < v \leq 70km/h$  | $S \geq 60m$    |
| Low speed      | $20km/h < v \leq 40km/h$  | $S \geq 30m$    |
| Slow speed     | $v \leq 20km/h$           | $S \geq 10m$    |

The relationship between  $v$  (vehicle speed,  $m/s$ ) and  $s$  (minimum safe distance,  $m$ ) can be obtained by linear fitting, as shown in Figure 4, and its formula is as follows:

$$s = 4.07v - 15.82 \quad (10)$$

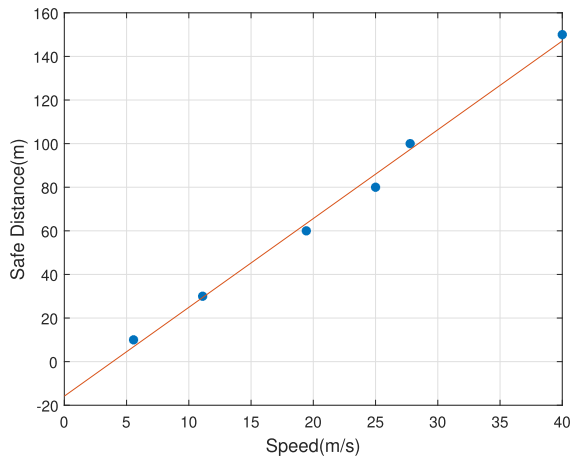


**FIGURE 4. Linear fitting of vehicle safety distance and speed.**

When there are multiple vehicles in the area, the maximum value of risk force shall be taken, including:

$$F'_{0i} = \max_{i \in \{1, 2, \dots, n\}} \{F_{0i}\} \quad (11)$$

$$F'_{max} = \max_{i \in \{1, 2, \dots, n\}} \{F_{max}\} \quad (12)$$

where,  $F'_{0i}$  and  $F'_{max}$  are the maximum values of  $F_{0i}$  and  $F_{max}$ , respectively.  $F'_{max}$  is independent of  $F'_{0i}$ , because of the driver's control of the vehicle in the actual driving. The driver's understanding of driving risks is not accurate enough, which may lead to  $F'_{max} < F'_{0i}$ . When it happens, the artificial setting of  $F'_{max} = F'_{0i}$  indicates that the vehicle is in a dangerous state.

## B. REAL TIME DELAY RATE AND REAL TIME LOAD RATE

### 1) DATA PRIORITY

An important feature of vehicle safety communication is that important safety information has higher real-time requirement and higher priority than general information. Therefore, IEEE 802.11p specifically adopts the EDCA mechanism and introduces QoS support, redefining four different Access Categories (AC). According to the importance and real-time of message content, EDCA assigns an AC to each frame generated by the application, and determines different AC through AC Index (ACI). Each AC has its own frame sequence and parameter set to coordinate media access [26].

At present, according to EDCA program, AC is divided into four types, represented by ACI, which are 0, 1, 2 and 3, respectively, corresponding to four types of information with different emergency degree and priority. The larger ACI is, the higher the emergency degree of information is and the higher the priority is. The frame of ACI = 0 is used for normal access medium, the frame of ACI = 1 is used for non-priority background traffic information, and the frame of ACI = 2 and 3 is reserved for priority information, such as danger and safety warning.

*Defination 1:* Data priority ( $\alpha$ ) to indicate the urgency of the current packet to be sent. The expression is as follows:

$$\alpha = \frac{ACI + 1}{ACNum + 1} \quad (13)$$

where, ACI represents the sending priority of the packet,  $ACI \in (0, 1, 2, 3)$ . The larger the ACI, the higher the data priority.  $ACNum$  is the number of ACI species, and in IoV environment, there are four kinds of ACI, so  $ACNum = 4$ . According to the definition, the value of ACI is 0, 1, 2 or 3, and the value of  $ACNum$  is 4. Therefore, it can be concluded that  $ACI < ACNum, \alpha \in (0, 1)$ .

### 2) REAL TIME DELAY RATE

Round-Trip Time (RTT) is the total delay of data message from the sender to the receiver. RTT is an important parameter to judge the transmission performance of data link. In multi-link network protocol, link selection is usually based on RTT, such as multipath TCP protocol [27], [28].

With the continuous development and application of heterogeneous network integration technology in the field of IoV, there are many different types of links in the communication nodes of IoV. For the link selection algorithm in the heterogeneous network fusion technology, it is very important to accurately judge the link state and distribute the upper layer data packets to the appropriate link for transmission. But for different types of links, the measurement standard of link state is quite different, for example, the same RTT, for Wi-Fi and 5G, two different types of links indicate that one is in good condition while the other is congested [29]. Therefore, the absolute value of RTT is not suitable to measure the state of different types of links in heterogeneous networks.

*Defination 2:* The real-time delay rate is used to represent the weight of the delay at a certain time of the link when



judging the data priority matching degree of the link. It is represented by  $RE_i(t)$ . The expression is as follows:

$$RE_i(t) = \frac{R_i(t)}{R_{i\max}} \quad (14)$$

where,  $R_i(t)$  represents the RTT of link  $i$  at time  $t$ ,  $R_{i\max}$  represents the maximum delay response tolerance time constant of link  $i$ , beyond which the message is considered to be lost. Apparently,  $R_i(t) > 0$ ,  $R_{i\max} > 0$ . It is obvious from the definition that when  $R_i(t) \leq R_{i\max}$ , the message is not lost, and  $RE_i(t) \in [0, 1)$ . When  $R_i(t) > R_{i\max}$ , the message is lost, then the value of  $RE_i(t)$  is 1. Therefore, the final value range of  $RE_i(t)$  is  $[0, 1]$ .

### 3) REAL TIME LOAD RATE

Link load is also one of the important parameters to measure the performance of link transmission, which is represented by the proportion of data messages in the transmission queue buffer. The larger the proportion is, the higher the link load is. Research on load balancing can improve link utilization and communication quality. There are many load balancing algorithms, such as polling method, weighted optimal path method and so on. The current algorithm is mainly used in the same type of multi-link scenarios, but in heterogeneous networks, the parameters of each link are often different. So it is not appropriate to distribute data by comparing the used size of the send queue buffer. Therefore, this paper uses the proportion of link load to represent the usage of link load, which can better reflect the load of heterogeneous links.

*Defination 3:* The real-time load rate refers to the weight of the load at a certain time of the link when judging the data priority matching degree of the link, which is represented by  $LE_i(t)$ . The expression is as follows:

$$LE_i(t) = \frac{L_i(t)}{L_{i\max}} \quad (15)$$

where,  $L_i(t)$  represents the load value of link  $i$  at time  $t$ , and  $L_{i\max}$  represents the upper bound on load of link  $i$ . If  $L_i(t) > L_{i\max}$ , it indicates that the transmission buffer of the link is full and congestion occurs, which means that the message is unable to send into the buffer. Therefore,  $L_i(t) \leq L_{i\max}$ .

According to the congestion theorem, the change of transmission buffer usage can be divided into two stages: growth stage and congestion stage. In the growth stage, the occupied interval of the transmit buffer increases all the time, but it does not reach the peak value. In this stage,  $L_i(t) < L_{i\max}$ ,  $LE_i(t) \in [0, 1)$ ; While in the congestion stage, the transmit buffer has been completely occupied, at this time,  $L_i(t) = L_{i\max}$ ,  $LE_i(t) = 1$ . Therefore, the value range of  $LE_i(t)$  is  $[0, 1]$ .

## C. INFORMATION TRANSMISSION FREQUENCY MODEL

### 1) THE TRANSMISSION FREQUENCY MODEL OF SAFETY INFORMATION BASED ON TRAFFIC RISK FIELD

The broadcasting frequency of status message stipulated by the current vehicle network communication protocol standard

is 1-10 Hz. The higher the frequency is, the more frequent the security message exchange of the vehicle is, and the safer the environment the vehicle is in.

Section 3A introduces the vehicle risk field model, in which the risk force can represent the risk level of the vehicle driving. When the vehicle risk is high, the transmission frequency of WSM is more frequent; when the vehicle risk is low, the transmission frequency of WSM is appropriately reduced to provide idle link resources for NWSM transmission.

The expression of WSM sending frequency  $f$  is:

$$f = \begin{cases} 1, & F'_{oi} = 0 \\ \left\lfloor \frac{F'_{oi}}{F'_{\max}} \times 10 \right\rfloor + 1, & 0 < F'_{oi} < F'_{\max} \\ 10, & F'_{oi} \geq F'_{\max} > 0 \end{cases} \quad (16)$$

where,  $F'_{oi}$  is the maximum risk force of the current vehicle 0 in the communication range, and  $F'_{\max}$  is the upper bound of risk force that the current vehicle can theoretically be suffered on the premise of safe driving. When  $F'_{oi} = 0$ , there is no vehicles in the communication range of the current vehicle 0. At the time, the vehicle 0 broadcasts status messages in accordance with the lowest frequency stipulated by the communication protocol standard in IoV, and  $f$  takes its minimum value of 1Hz. When  $0 < F'_{oi} < F'_{\max}$ ,  $\frac{F'_{oi}}{F'_{\max}} < 1$ , the value range of  $f$  is  $[1, 10]$ . When  $F'_{oi} \geq F'_{\max} > 0$ , taking  $F'_{\max} = F'_{oi}$  indicates that the vehicle is in a dangerous state according to the analysis of formula (11) and (12) in Section 3A, and  $f$  takes its maximum value of 10Hz. Therefore, the value range of  $f$  is  $[1, 10]$ .

### 2) THE TRANSMISSION FREQUENCY MODEL OF NON-SAFETY INFORMATION BASED ON PARETO OPTIMALITY

Pareto optimality is the ideal state of resource allocation, which means to make at least one person better in the change from one allocation state to another without making anyone worse.

In the environment of IoV, both safety and non-safety messages need to compete for network resources. In order to ensure the safe driving, the transmission efficiency of non-safety messages should be improved on the premise of ensuring the transmission of safety messages. The optimal solution is Pareto optimal solution.

WSM has periodicity and the transmission frequency of it is 1-10Hz. In a WSM transmission period,  $c$  (the maximum number of NWSM that can be sent by IEEE 802.11p link) is:

$$c = \frac{T}{f(t)} \quad (17)$$

where,  $f(t)$  is the real-time transmission frequency of WSM, and  $T$  is the maximum throughput of IEEE 802.11p link.

In an ideal state, after sending non-WSM of  $c$  size, the next WSM can be sent directly without waiting and affecting the sending requirements of WSM.

Therefore, in practice, the maximum NWSM distribution frequency of IEEE 802.11p link can be obtained by judging whether the remaining space of MAC layer transmit buffer is larger than that of  $c$ ,

$$f_{u\max} = \begin{cases} T, & L_{\max} - L_{80211p}(t) \geq c \\ (L_{\max} - L_{80211p}(t)) \cdot f(t), & L_{\max} - L_{80211p}(t) < c \end{cases} \quad (18)$$

where  $L_{\max}$  is the transmission buffer size of the IEEE 802.11p link, and  $L_{80211p}(t)$  is the transmission buffer size currently used by the IEEE 802.11p link. It is known from formula (18) that when the NWSM distribution frequency of IEEE 802.11p link reaches  $f_{u\max}$ , WSM and NWSM achieve Pareto optimality, and both parties obtain the maximum transmission benefit.

### 3) SECURITY INFORMATION TRAFFIC ESTIMATION MODEL

Network performance is related to the current vehicle mobile environment in IoV. At present, IEEE 802.11p is the communication protocol used in the data link layer MAC sub-layer of the Internet of vehicles. In the cooperative vehicle security system, a single vehicle state message exchange will cause congestion in the control channel of IEEE 802.11p and degrade the network performance.

According to the relevant research, the vehicle mobile environment has an important impact on the performance of IEEE 802.11p protocol. According to IEEE 802.11p protocol, vehicle status messages will be transmitted between vehicles in the way of periodic broadcast. When the vehicle is congested, the IEEE 802.11p channel will increase the load due to many such messages, and the packets will collide. Statistically, when there are 360 vehicles in the communication range and the packet transmission rate is 10 *packets/s*, the packet loss rate is as high as 71% [30]. Currently, it is necessary to reduce the amount of packet transmission to ensure network performance. However, in the case of sparse vehicles, the distribution density of state messages between vehicles will decrease. When the vehicle makes a high-risk operation such as overtaking, accidents may occur due to the lack or delay of state messages. Therefore, this kind of security related messages need higher priority to meet the real-time requirements.

According to the properties of the IEEE 802.11p protocol mentioned above, this paper proposes a traffic flow density-based traffic volume estimation of the nodes in IoV to ensure the transmission performance of the IEEE 802.11p link. The estimated traffic volume between a vehicle  $i$  and other vehicles at time  $t$  can be obtained by the following formula (19):

$$T_i = \sum_{j=1}^N f(t)_j \cdot A_j \quad (19)$$

where,  $f(t)$  is the broadcast frequency of vehicle status message specified in IEEE 802.11p protocol

between 1-10Hz. According to different vehicle operation conditions, it demonstrates different driving risks. The higher the risk of vehicle operation environment, the more frequent the exchange of safety messages together with the higher the transmission frequency.  $A$  refers to the number of safety applications running in the current vehicle,  $N$  refers to the number of vehicles within the communication range,  $f(t) \cdot A$  refers to the estimated traffic volume of a single vehicle at time  $t$ , and  $T_i$  refers to the total traffic volume between the current vehicle and other vehicles at time  $t$ , including the actual traffic volume and potential traffic volume.

## IV. INTRODUCTION TO LLCA ALGORITHM

### A. DATA PRIORITY WEIGHT OF LINK

(1) Gets the data type. Whenever the vehicle wants to send data, the data packet will be transferred down to the LLC layer. At this time, the LLC layer will judge the data type according to the priority of the data packet. If the data packet is WSM, the data packet will be directly allocated to the link using IEEE 802.11p protocol for transmission, to ensure the transmission requirements of the security message and the QoE of the security applications.

If the data packet delivered to LLC layer is the traditional TCP/IP packet, that is, the insecure packet, then it is necessary to judge and analyze the current status of the link, and select the link most suitable for the packet for transmission.

(2) The data link weight (DPW) indicates the matching degree of the link to the current packet at a certain time. As shown in formula (20).

$$s_i(t) = \begin{cases} (1 - \alpha_p)RE_i(t) + \alpha_p \cdot LE_i(t), & \text{other link} \\ (1 - \alpha_p)RE_i(t) + \alpha_p \cdot \frac{L_i(t)}{L_{i\max} - x(t)}, & \text{IEEE 802.11p} \end{cases} \quad (20)$$

where  $s_i(t)$  represents the DPW value of link  $i$  with respect to packet  $p$  at time  $t$ ,  $\alpha_p$  is the priority of non-safety type packet  $p$ ,  $RE_i(t)$  and  $LE_i(t)$  are the RTT and link load factor of link  $i$  at time  $t$  respectively, and  $x(t)$  is the current safety information traffic volume estimation of the vehicle. In IoV, the state information of vehicles will be exchanged between vehicles to ensure the safety of vehicle driving. At the same time, in order to spread the state of vehicles to the whole network, vehicles will forward the received safety data of other vehicles to ensure the consistency of the whole Internet of vehicles and the instantaneity of current data. Therefore, in order to ensure the transmission demand of safety information, when calculating the DPW value of IEEE 802.11p link, it is necessary to subtract the current estimated value of vehicle safety information traffic from the denominator part of the link load factor as the reserved space for the interaction and forwarding of vehicle safety information. In general, there is  $L_{i\max} > x(t)$ . When the traffic environment is extremely congested, there may be  $L_{i\max} < x(t)$ , and  $s_i(t) > x(t)$ . When  $\frac{L_i(t)}{L_{i\max} - x(t)} > 1$ , take  $\frac{L_i(t)}{L_{i\max} - x(t)} = 1$ . According to formula (20), the DPW value of all links is calculated, and

the link with the lowest DPW value is selected to allocate the packet  $p$  to the corresponding link.

(3) Calculates the maximum distribution frequency of packets of non-security type. After the above two steps, if the data packet  $p$  is allocated to the IEEE 802.11p link, then the maximum NWSM distribution frequency  $f_{umax}$  of the IEEE 802.11p link needs to be calculated by formula (18), and then the instantaneous distribution frequency  $f_u$  of the IEEE 802.11p link needs to be calculated by using the two adjacent NWSM that arrive at the latest IEEE 802.11p link.

$$f_u = \frac{1}{t_2 - t_1} \quad (21)$$

where  $t_1$  and  $t_2$  are the time when two adjacent NWSM reach the IEEE 802.11p link respectively.

Finally, the comparison between  $f_u$  and  $f_{umax}$  is used. If  $f_u < f_{umax}$ , the distribution is successful; if  $f_u > f_{umax}$ , the distribution fails, and the packet enters the waiting queue of LLC layer and waits for distribution again.

The process of LLCA algorithm is shown in Figure 5.

### Algorithm 1 LLCA

```

1 While(TURE)
2   Priority = packet.getPriority();
3   If (Priority == 3)
4     sendPkt(packet, link80211p)
5   else
6     s1 = getLinkS(link80211p, Priority)
7     s2 = getLinkS(linkLTE, Priority)
8     If (s1 < s2)
9       uMaxF = maxdistFreq(link80211p)
10      uF = nowdistFreq(packet1, packet2)
11      If (uF < uMaxF)
12        sendPkt(packet, link80211p)
13      else
14        backToQueue(packet)
15      end if
16    else
17      sendPkt(packet, linkLTE)
18    end if
19  end if
    
```

### B. PERFORMANCE ANALYSIS OF LLCA ALGORITHM

*Theorem 1:* When there are  $n$  links and  $m$  cars in the system, the worst time complexity of LLCA algorithm is  $O(m + n)$ .

*Proof:* The LLCA algorithm has a simple structure and only one cycle. When there are  $m$  cars in the system, the time complexity required for the algorithm to calculate the risk forces of all cars is  $O(m)$ . In the worst case, the algorithm needs to scan all the links, calculate the DPW value of all links and find out the minimum value. When there are  $n$  links in the system, in the worst case, the time complexity required for the algorithm to scan all links to calculate the DPW value of each link is  $O(n)$ , and the time complexity required to find the minimum value among  $n$  DPW values is also  $O(n)$ . Therefore,

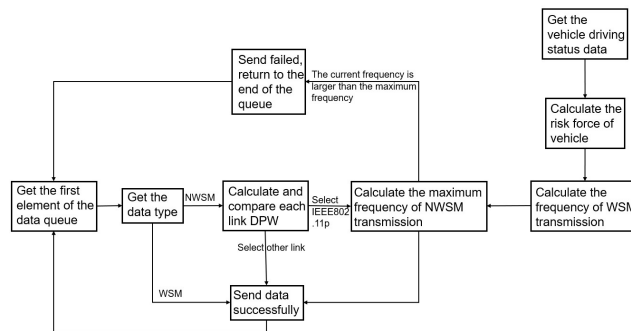


FIGURE 5. Process of LLCA.

the time complexity of LLCA algorithm in the worst case is  $O(m) + O(n) + O(n)$ , that is, the worst time complexity of LLCA algorithm is  $O(m + n)$ .

*Theorem 2:* LLCA algorithm satisfies Pareto optimality.

*Proof:* according to the description in Section 4A, under the control of LLCA, the transmission frequency  $f_u$  of NWSM datagram on IEEE 802.11p link meets the requirement of  $f_u \leq f_{umax}$ . If  $f_u = f_{umax}$ , combined with the analysis of Section 3C, it can be seen that WSM and NWSM meet the Pareto optimization; if  $f_u < f_{umax}$ , it means that the speed of sending NWSM on IEEE 802.11p link is faster than that of sending NWSM on LLC layer to IEEE 802.11p link, at this time, all data packets can be sent directly without waiting, and at this time, LLCA still meets the Pareto optimization.

## V. EXPERIMENTAL SIMULATION AND PERFORMANCE ANALYSIS

### A. EXPERIMENTAL SCENARIOS AND DATA SAMPLES

In this paper, Visual Studio 2017 is used to simulate the multi-link communication environment, Simulation of Urban MObility (SUMO) traffic simulation software is used to simulate the actual road traffic scene, and different WSM traffic volume is set according to different vehicle congestion degree in IoV environment to verify the performance of LLCA algorithm. The performance of LLCA algorithm is compared with Polling algorithm (PA) used in reference [31] CSVSM algorithm (Collaborative SVC Video Streaming Methods) proposed in reference [32] for performance analysis and comparison. Because this paper mainly studies the implementation of heterogeneous network convergence on LLC layer, which is transparent to the upper layer network protocol, the implementation of the upper layer protocol is not demonstrated in this section. Using Visual Studio 2017 simulation environment, we can ignore the unnecessary details, focus on the parts that need to be modified, and reduce the difficulty of implementation.

In the multi-channel protocol, based on the polling mechanism, which is widely used in multichannel protocol, PA algorithm allocates packets to each link in turn for transmission, to achieve load balancing. CSVSM algorithm is designed for the link scheduling of IoV. The algorithm schedules and distributes different packets for IEEE 802.11p link and LTE link, that is, use IEEE 802.11p link to transmit WSM and

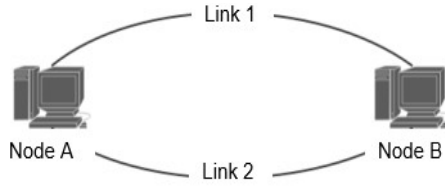


FIGURE 6. Experimental simulation model.

LTE link to transmit NWSM packets, such as video stream packets.

The simulation model is shown in Figure 6, which was mentioned in reference [33]. Link 1 is IEEE 802.11p link, and Link 2 is LTE link. The parameters of the link are shown in Table 2:

In this experiment, the above two algorithms are tested as comparison algorithms. The test process is as follows: in the PA algorithm, Node A will transmit the WSM directly through Link 1, and the NWSM will be distributed to two links in turn for transmission; in the CSVSM algorithm, Link 1 as the exclusive channel only transmits the WSM, and Link 2 only transmits the NWSM.

According to the different traffic environment, this experiment sets up three different levels of vehicle congestion corresponding to the sparse, normal and congested traffic flow, respectively. As mentioned above, the exchange of vehicle

TABLE 2. Links parameters.

| Parameter               | Value |
|-------------------------|-------|
| Link 1 delay/ms         | 10    |
| Link 1 send buffer size | 500   |
| Link 2 delay /ms        | 50    |
| Link 2 send buffer size | 500   |

status message (WSM) between vehicles is required to ensure the safe driving of vehicles. Therefore, the more congested the traffic flow, the higher the frequency of WSM transmission between vehicles, and the larger proportion of WSM in all data. So, in this experiment, we adjust the proportion of WSM in the whole data sample to reflect the different traffic density.

For the size of the experimental sample, 6000 data packets are set in this experiment. According to EDCA mechanism, four kinds of data packets with different priority are randomly generated, among which WSM is the highest priority data packet. According to the actual driving conditions of vehicles, it can be divided into three driving conditions: sparse, normal and congested, representing the vehicle scale within the communication range, with corresponding coefficients of 100, 300, 500. The design idea is: when there are many vehicles in the communication range, but the vehicle distance is long, the vehicle risk is not high, that is, the WSM transmission frequency is low; when there are few vehicles in the

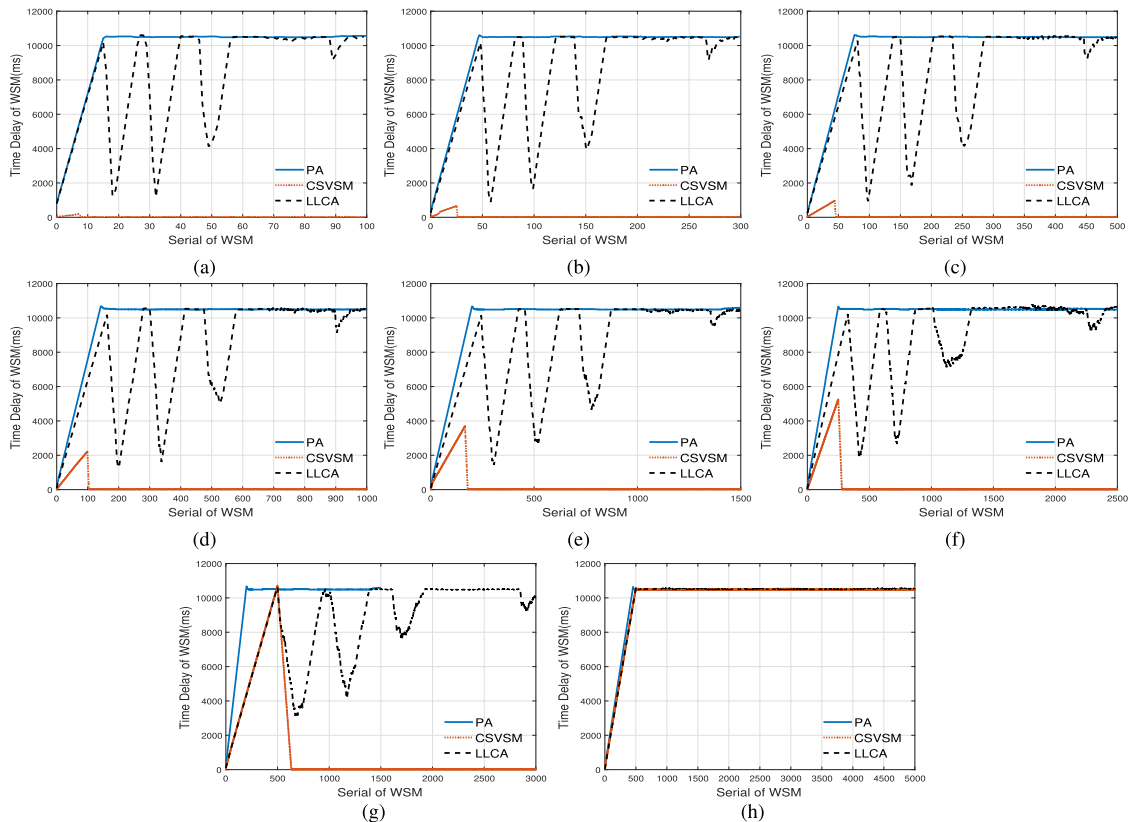


FIGURE 7. WSM delay under different WSM traffic. (a)  $Q_{WSM} = 100$  (b)  $Q_{WSM} = 300$  (c)  $Q_{WSM} = 500$  (d)  $Q_{WSM} = 1000$  (e)  $Q_{WSM} = 1500$  (f)  $Q_{WSM} = 2500$  (g)  $Q_{WSM} = 3000$  (h)  $Q_{WSM} = 5000$ .



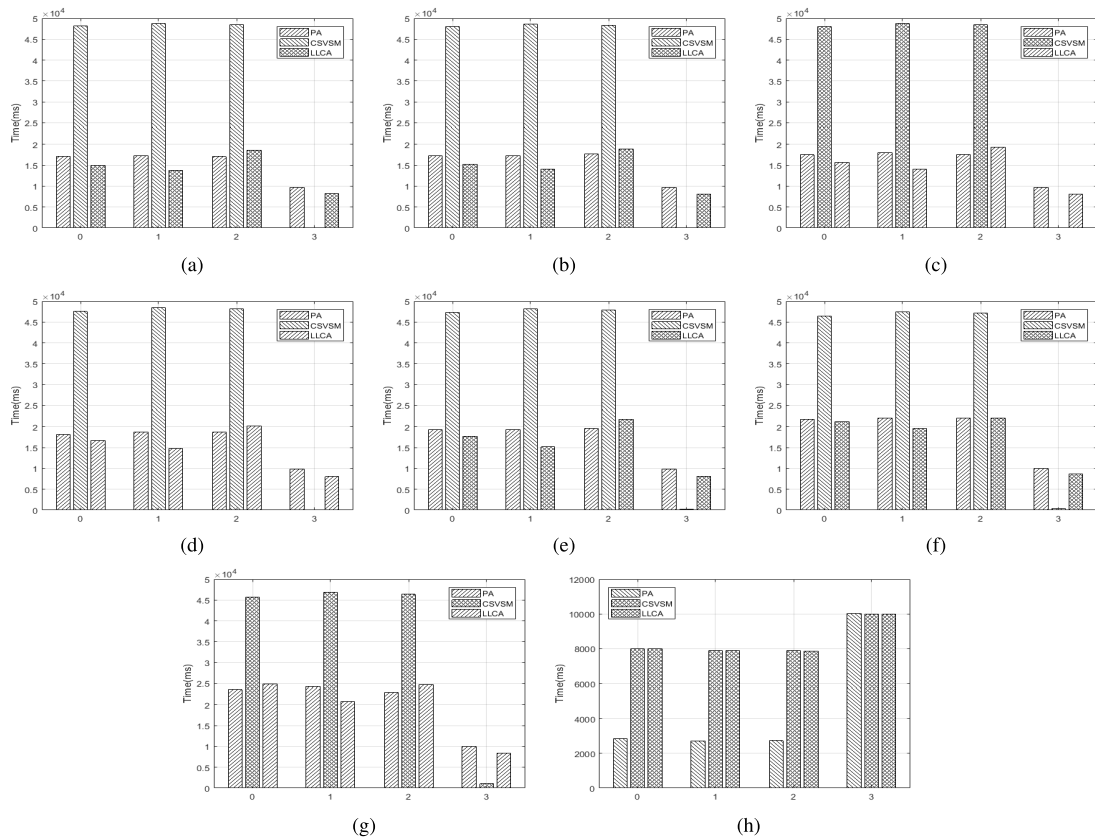


FIGURE 8. Average delay of each priority packets under different WSM traffic. (a)  $Q_{WSM} = 100$  (b)  $Q_{WSM} = 300$  (c)  $Q_{WSM} = 500$  (d)  $Q_{WSM} = 1000$  (e)  $Q_{WSM} = 1500$  (f)  $Q_{WSM} = 2500$  (g)  $Q_{WSM} = 3000$  (h)  $Q_{WSM} = 5000$ .

TABLE 3. WSM estimated traffic.

| WSM Estimated traffic<br>$Q_{WSM}$ |    | Traffic Size Estimates $S$ |            |               |
|------------------------------------|----|----------------------------|------------|---------------|
|                                    |    | Sparse/100                 | Normal/300 | Congested/500 |
| WSM                                | 1  | 100                        | 300        | 500           |
| Transmission                       | 5  | 500                        | 1500       | 2500          |
| Frequency $f$                      | 10 | 1000                       | 3000       | 5000          |

communication range, but the vehicle distance is very close, the vehicle risk is high, that is, the WSM transmission frequency is high. Therefore, the WSM estimated traffic,  $Q_{WSM}$  is jointly determined by WSM transmission frequency  $f$  and traffic flow estimation  $S$ , as shown in formula (22).

$$Q_{WSM} = f \cdot S \tag{22}$$

As mentioned above, the WSM estimated traffic in this experiment are shown in Table 3.

### B. COMPARISON AND ANALYSIS OF WSM TRANSMISSION PERFORMANCE

Figure 7 shows the transmission delay of WSM under different WSM estimates. It can be seen from Figure 7 that in the case of sparse, normal and congestion, the WSM transmission delay of LLCA is smaller than PA and larger than CSVSM. In addition, when the link is congested, LLCA will dynamically adjust the load of the link, to reduce the congestion

TABLE 4. IEEE 802.11p link utilization under different wsm traffic.

| Link IEEE 802.11p utilization |      | Algorithm |        |        |
|-------------------------------|------|-----------|--------|--------|
|                               |      | PA        | CSVSM  | LLCA   |
| WSM Traffic<br>$Q_{WSM}$      | 100  | 88.47%    | 0.25%  | 74.36% |
|                               | 300  | 88.24%    | 0.46%  | 73.89% |
|                               | 500  | 88.38%    | 0.58%  | 73.90% |
|                               | 1000 | 88.87%    | 1.25%  | 74.20% |
|                               | 1500 | 89.32%    | 2.28%  | 74.18% |
|                               | 2500 | 90.87%    | 2.85%  | 78.74% |
|                               | 3000 | 90.22%    | 10.59% | 76.43% |
|                               | 5000 | 91.21%    | 90.73% | 90.90% |

of the link, ensure that the link is in a relatively good state and reduce the transmission delay of WSM. As mentioned above, WSM can only be transmitted through IEEE 802.11p link, so it can be seen from Figure 7 that when the traffic environment is more congested and the distance between vehicles is very close, the performance of the three algorithms is similar, because the number of WSM transmitted through IEEE 802.11p link is much more than other types of packets. When the traffic density reaches its extreme, that is, when the proportion of WSM in the total packets reaches nearly 80%, the transmission performance of the three algorithms is almost the same.

It can also be seen from the result that in the non-extreme case, the WSM delay of CSVSM is lower than that of

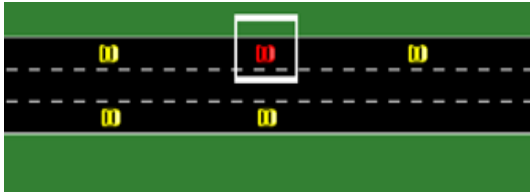


FIGURE 9. SUMO simulation traffic scene.

PA and LLCA. This is because the frequency of generating WSM is lower when the traffic flow is not dense. In CSVSM, the IEEE 802.11p link is only responsible for WSM transmission, so the IEEE 802.11p link will not be congested. The WSM delay will be relatively low, but CSVSM low delay is achieved at the expense of many link resources.

C. COMPARATIVE ANALYSIS OF LINK UTILIZATION

Table 4 shows the utilization ratio of IEEE 802.11 link under different communication traffic scales.

It can be seen from Table 4 that PA has the highest utilization rate of IEEE 802.11p link in general, which is over 90%. However, it can be seen from Figure 7 that PA will cause IEEE 802.11p link to be congested for a long time and increase the delay of WSM. From Figure 7 and Table 4, the low delay of CSVSM algorithm for WSM is obtained at the cost of low utilization of IEEE 802.11p link. In general, CSVSM’s utilization of IEEE 802.11p link is less than 2% and less than 1% in the case of sparse traffic flow, which is undoubtedly a great waste of network resources. LLCA adjusts IEEE dynamically the load of 802.11p link can not only guarantee the delay of WSM at a low level, but also keep the utilization of IEEE 802.11p link at about 70%. In the case of extremely dense traffic flow, the utilization ratio of the three algorithms for IEEE 802.11p link is basically the same, reaching over 93%, which is consistent with the situation shown in Figure 7-(h). It shows that the performance of the three algorithms is closer with the increase of WSM traffic.

D. COMPARATIVE ANALYSIS OF TRANSMISSION PERFORMANCE OF PRIORITY PACKETS

In order to reflect the impact of LLCA on the overall transmission performance of the network, this section makes statistics on the average delay of all different types of data packets, and compares the differences between the three algorithms in the overall transmission performance, as shown in Figure 8.

It can be seen from Figure 8 that in the case of sparse, normal and congestion traffic, CSVSM algorithm will increase the delay of low priority packets, which is much larger than that of PA and LLCA, while the average transmission delay of low priority packets of LLCA is basically smaller than that of PA and CSVSM; in the case of extremely dense traffic flow, the low priority datagram of PA algorithm will use IEEE 802.11p link to transmit, while IEEE 802.11p link has larger bandwidth than LTE link, and transmission delay is smaller than LTE link, which makes the average

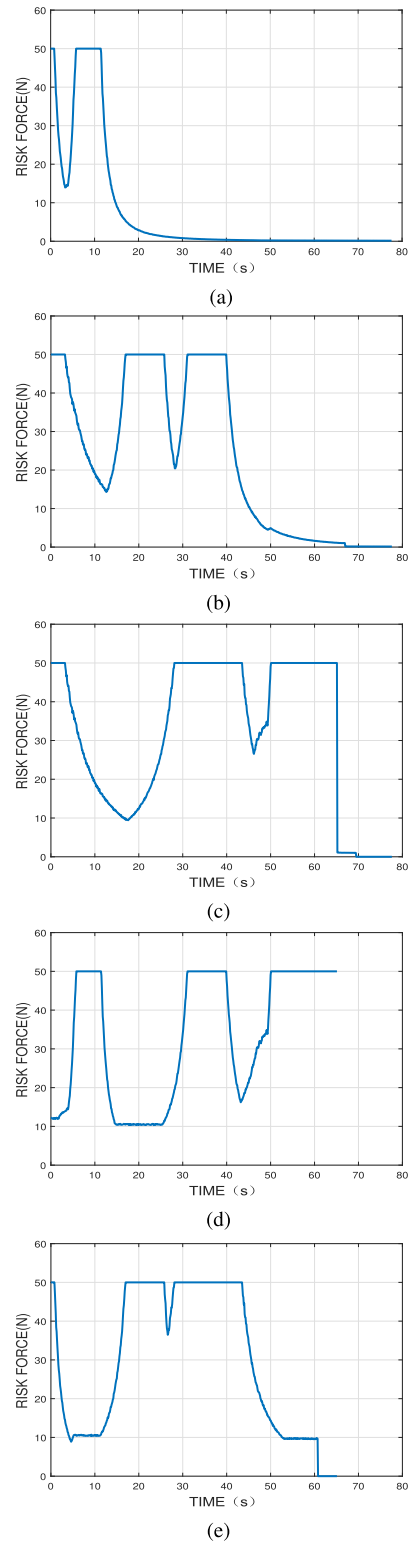
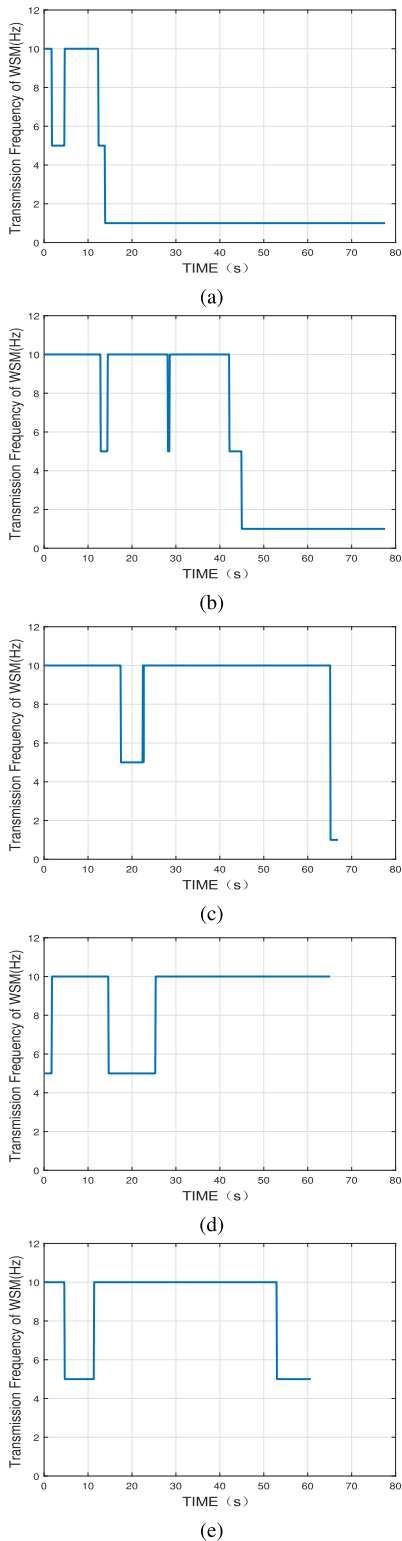


FIGURE 10. Variation of vehicle risk intensity. (a) CAR 1 (b) CAR 2 (c) CAR 3 (d) CAR 4 (e) CAR 5.

delay of low priority packets in PA algorithm smaller than CSVSM and LLCA, and leads to the average delay of WSM (priority 3) in PA larger than CSVSM and LLCA. Based on the above comparison and analysis, it can be concluded that



**FIGURE 11.** Variation of WSM transmission frequency. (a) CAR 1 (b) CAR 2 (c) CAR 3 (d) CAR 4 (e) CAR 5.

LLCA can not only reduce the transmission delay of WSM and improve the utilization of link resources, but also reduce the transmission delay of other types of data packets, meet the

QoE of various types of applications, and improve the overall transmission performance of the Internet of vehicles.

### E. RELATIONSHIP ANALYSIS BETWEEN VEHICLE RISK FORCE AND WSM TRANSMISSION FREQUENCY BASED ON SUMO

This part uses SUMO traffic simulation software to build a two-lane traffic scene, and then simulate the traffic situation in the real scene. The scene settings are shown in Figure 9.

From the beginning of vehicle entering the scene to the end of vehicle leaving the scene, collect the driving status of vehicles in the area every 0.1 seconds. As the vehicle runs, the risk intensity of each vehicle changes, as shown in Figure 10. The corresponding WSM transmission frequency is shown in Figure 11.

Based on the data obtained from SUMO scenario, the algorithm proposed in this paper is further tested. The experimental results are shown in the Figure 10 and Figure 11. As can be seen from the chart, the simulation results based on the actual scene are basically consistent with the results in the previous section. LLCA algorithm allows some low priority data packets to be transmitted via IEEE 802.11p link, so it reduces the transmission performance of WSM. In addition, with the dynamic adjustment based on link state and traffic density, the transmission performance of WSM is still stable. The experimental results show that the algorithm improves the utilization of IEEE 802.11p link and improves the transmission performance of low priority data packets.

### VI. CONCLUSION

On the basis of analyzing the existing heterogeneous network fusion research, this paper establishes the risk field model of vehicle driving, and proposes LLCA, a heterogeneous network link scheduling algorithm based on priority, link state and traffic flow density, according to the transmission requirements of security services in the Internet of vehicles system. The link scheduling algorithm proposed in this paper is to guarantee the QoE of non-secure services on the premise of satisfying the transmission requirements of security services first, and meanwhile to use event-triggered mechanism to carry out unified management of link resources in IoV, such that improve the utilization rate of link resources can be improved. Simulation results show that compared with other link scheduling algorithms, the improved algorithm can effectively reduce the average transmission delay of WSM in IoV and improve the average utilization rate of the link, and further improve the overall performance of IoV.

The structure of vehicle-risk-field model needs more details of vehicles like steering angle and braking distance. The combination of vehicle-risk-field assessment method with V2V communication is required to get further research. In heterogeneous network fusion, switching between different networks often leads to delay, packet loss, or extra communication overhead, which need to be considered in further optimization.

## REFERENCES

- [1] W. Liu and Y. Shoji, "DeepVM: RNN-based vehicle mobility prediction to support intelligent vehicle applications," *IEEE Trans. Ind. Informat.*, vol. 16, no. 6, pp. 3997–4006, Jun. 2020.
- [2] E. Sisinni, A. Saifullah, S. Han, U. Jennehag, and M. Gidlund, "Industrial Internet of Things: Challenges, opportunities, and directions," *IEEE Trans. Ind. Informat.*, vol. 14, no. 11, pp. 4724–4734, Nov. 2018.
- [3] C. Lu, A. Saifullah, B. Li, M. Sha, H. Gonzalez, D. Gunatilaka, C. Wu, L. Nie, and Y. Chen, "Real-time wireless sensor-actuator networks for industrial cyber-physical systems," *Proc. IEEE*, vol. 104, no. 5, pp. 1013–1024, May 2016.
- [4] Z. Ning, Y. Li, P. Dong, X. Wang, M. S. Obaidat, X. Hu, L. Guo, Y. Guo, J. Huang, and B. Hu, "When deep reinforcement learning meets 5G-enabled vehicular networks: A distributed offloading framework for traffic big data," *IEEE Trans. Ind. Informat.*, vol. 16, no. 2, pp. 1352–1361, Feb. 2020.
- [5] E. Ahmed and H. Gharavi, "Cooperative vehicular networking: A survey," *IEEE Trans. Intell. Transp. Syst.*, vol. 19, no. 3, pp. 996–1014, Feb. 2018.
- [6] Y. Kim, M. Lee, and T.-J. Lee, "Coordinated multichannel MAC protocol for vehicular ad hoc networks," *IEEE Trans. Veh. Technol.*, vol. 65, no. 8, pp. 6508–6517, Aug. 2016.
- [7] A. Sarker, H. Shen, and J. A. Stankovic, "MORP: Data-driven multi-objective route planning and optimization for electric vehicles," in *Proc. ACM Interact., Mobile, Wearable Ubiquitous Technol.*, 2017, pp. 1–35.
- [8] C. Xu, F. Zhao, J. Guan, H. Zhang, and G.-M. Muntean, "QoE-driven user-centric VoD services in urban multihomed P2P-based vehicular networks," *IEEE Trans. Veh. Technol.*, vol. 62, no. 5, pp. 2273–2289, Jun. 2013.
- [9] S.-L. Tsao and C.-M. Cheng, "Design and evaluation of a two-tier peer-to-peer traffic information system," *IEEE Commun. Mag.*, vol. 49, no. 5, pp. 165–172, May 2011.
- [10] R. Trestian, I. S. Comsa, and M. F. Tuysuz, "Seamless multimedia delivery within a heterogeneous wireless networks environment: Are we there yet?" *IEEE Commun. Surveys Tuts.*, vol. 41, no. 1, pp. 945–977, 1st Quart., 2018.
- [11] Y. Thomas, M. Karaliopoulos, G. Xylomenos, and G. C. Polyzos, "Low latency friendliness for multipath TCP," *IEEE/ACM Trans. Netw.*, vol. 28, no. 1, pp. 248–261, Jan. 2020.
- [12] W. Wei, K. Xue, J. Han, D. S. L. Wei, and P. Hong, "Shared bottleneck-based congestion control and packet scheduling for multipath TCP," *IEEE/ACM Trans. Netw.*, vol. 28, no. 2, pp. 653–666, Apr. 2020.
- [13] K. Zheng, Q. Zheng, P. Chatzimisios, W. Xiang, and Y. Zhou, "Heterogeneous vehicular networking: A survey on architecture, challenges, and solutions," *IEEE Commun. Surveys Tuts.*, vol. 17, no. 4, pp. 2377–2396, 4th Quart., 2015.
- [14] K. Abbas, K. T. Ahmed, A. Rafiq, W.-C. Song, and S.-J. Seok, "An LTE-WiFi spectrum aggregation system for 5G network: A testbed," in *Proc. Int. Conf. Inf. Netw. (ICOIN)*, Jan. 2020, pp. 1–3.
- [15] K. J. S. White, E. Denney, M. D. Knudson, A. K. Mamerides, and D. P. Pezaros, "A programmable SDN+ NFV-based architecture for UAV telemetry monitoring," in *Proc. 14th IEEE Annu. Consum. Commun. Netw. Conf. (CCNC)*, Jan. 2017, pp. 522–527.
- [16] C. Chen, L. Liu, T. Qiu, D. O. Wu, and Z. Ren, "Delay-aware grid-based geographic routing in urban VANETs: A backbone approach," *IEEE/ACM Trans. Netw.*, vol. 27, no. 6, pp. 2324–2337, Dec. 2019.
- [17] F. Tao, J. Cheng, and Q. Qi, "IIHub: An industrial Internet-of-Things hub toward smart manufacturing based on cyber-physical system," *IEEE Trans. Ind. Informat.*, vol. 14, no. 5, pp. 2271–2280, May 2018.
- [18] D. Ni, "A unified perspective on traffic flow theory, part I: The field theory," *Appl. Math. Sci.*, vol. 65, no. 87, pp. 1929–1946, 2013.
- [19] C. Peng and F. Li, "A survey on recent advances in event-triggered communication and control," *Inf. Sci.*, vols. 457–458, pp. 113–125, Aug. 2018.
- [20] R. Matsumi, P. Raksincharoensak, and M. Nagai, "Autonomous braking control system for pedestrian collision avoidance by using potential field," *IFAC Proc. Vols.*, vol. 46, no. 21, pp. 328–334, 2013.
- [21] T. Sattel and T. Brandt, "From robotics to automotive: Lane-keeping and collision avoidance based on elastic bands," *Vehicle Syst. Dyn.*, vol. 46, no. 7, pp. 597–619, Jul. 2008.
- [22] J. Wang, J. Wu, and Y. Li, "The driving safety field based on driver-vehicle-road interactions," *IEEE Trans. Intell. Transp. Syst.*, vol. 16, no. 4, pp. 2203–2214, Feb. 2015.
- [23] *Responsibility-Sensitive Safety: A Mathematical Model for Automated Vehicle Safety*. Accessed: Apr. 30, 2020. [Online]. Available: <https://www.mobiley.com/responsibility-sensitive-safety/>
- [24] *Planning a Safer Path-Mathematically Verified and Validated in Simulation, NVIDIA Safety Force Field Protects Against Real-World Traffic*. Accessed: Apr. 30, 2020. [Online]. Available: <https://www.nvidia.com/en-us/self-driving-cars/safety-force-field/>
- [25] B. Y. L. Kimura, D. C. S. F. Lima, and A. A. F. Loureiro, "Packet scheduling in multipath TCP: Fundamentals, lessons, and opportunities," *IEEE Syst. J.*, early access, Jan. 27, 2020, doi: [10.1109/JSYST.2020.2965471](https://doi.org/10.1109/JSYST.2020.2965471).
- [26] *Wireless Access in Vehicular Environments*, IEEE Computer Society, IEEE Standard 802.11p TM-2010, 2010.
- [27] *Multipath TCP(MPTCP) Project*. Accessed: Apr. 30, 2020. [Online]. Available: <https://www.multipath-tcp.org/>
- [28] R. Hotchi and R. Kubo, "Active queue management supporting TCP flows using dynamically controlled target queue length," in *Proc. IEEE Int. Conf. Consum. Electron.-Taiwan (ICCE-TW)*, May 2018, pp. 1–2.
- [29] M. Yan, K.-Y. Lam, S. Han, E. Chan, Q. Chen, P. Fan, D. Chen, and M. Nixon, "Hypergraph-based data link layer scheduling for reliable packet delivery in wireless sensing and control networks with end-to-end delay constraints," *Inf. Sci.*, vol. 278, pp. 34–55, Sep. 2014.
- [30] J. B. Kenney, G. Bansal, and C. E. Rohrs, "LIMERIC: A linear message rate control algorithm for vehicular DSRC systems," in *Proc. 8th ACM Int. Workshop Veh. Inter-Netw. (VANET)*, Sep. 2011, pp. 21–30.
- [31] S. Barker, D. Irwin, and P. Shenoy, "Pervasive energy monitoring and control through low-bandwidth power line communication," *IEEE Internet Things J.*, vol. 4, no. 5, pp. 1349–1359, Oct. 2017.
- [32] E. Yaacoub, F. Filali, and A. Abu-Dayya, "QoE enhancement of SVC video streaming over vehicular networks using cooperative LTE/802.11p communications," *IEEE J. Sel. Topics Signal Process.*, vol. 9, no. 1, pp. 37–49, Feb. 2015.
- [33] Q. Peng, A. Walid, and S. H. Low, "Multipath TCP algorithms: Theory and design," in *Proc. ACM SIGMETRICS/Int. Conf. Meas. Modeling Comput. Syst. (SIGMETRICS)*, 2013, pp. 305–316.



**NAN DING** (Member, IEEE) was born in 1978. He received the B.S., M.S., and Ph.D. degrees in computer science from the Dalian University of Technology, Dalian, China, in 2002, 2005, and 2011, respectively.

He was a Visiting Scholar with the Electrical and Computer Engineering, University of New York University, USA, from September 2013 to September 2014. He has been an Associate Professor of computer science and engineering with the Dalian University of Technology. He has also been a Researcher with the State Key Laboratory of Software Architecture (Neusoft Corporation), Dalian. His research interests include vehicular networks, wireless security, wireless sensor networks, cache management, and distributed fault tolerant computing.



**SHAOHUA CUI** was born in 1997. She received the B.S. degree in computer science and technology from the Dalian University of Technology, Dalian, China, in 2019, where she is currently pursuing the M.S. degree in computer science.

Her research interests include industrial Internet of Things (IIoT), time-sensitive networks (TSNs), and multi-link scheduling.



**CHUANGUO ZHAO** was born in 1991. He received the B.S. degree in electronic and information engineering from the Dalian University of Technology, Dalian, China, in 2014, where he is currently pursuing the M.S. degree in computer science.

His research interests include vehicular networks and vehicle communication algorithm.





**YANHONG WANG** was born in 1998. She received the B.S. degree in computer science and technology from the Dalian University of Technology, Dalian, China, in 2016, where she is currently pursuing the M.S. degree in computer science and technology.

Her research interests include heterogeneous networks and time-sensitive networks (TSNs).



**BINGCAI CHEN** (Member, IEEE) received the M.S. and Ph.D. degrees in information and communication engineering from the Harbin Institute of Technology, Harbin, China, in 2003 and 2007, respectively.

He had been a Visiting Scholar with UBC, Canada, in 2015. He is currently a Professor with the School of Computer Science and Technology, Dalian University of Technology, and with the School of Computer Science and technology, Xinjiang Normal University. His research interests include wireless ad hoc networks, network and information security, and computer vision.

• • •